Macromolecules

Article

pubs.acs.org/Macromolecules

Thermoresponsive Amphiphilic Janus Silica Nanoparticles via Combining "Polymer Single-Crystal Templating" and "Grafting-from" Methods

Tian Zhou, Bingbing Wang, Bin Dong, and Christopher Y. Li*

Department of Materials Science and Engineering, Drexel University, Philadelphia, Pennsylvania 19104, United States

ABSTRACT: A facile method of synthesizing amphiphilic Janus silica nanoparticles (SiNPs) with bicompartment polymer brushes is presented in this article by combining "polymer single-crystal templating" (PSCryT) and "grafting from" techniques. First, alkoxysilane-terminated poly(ε-caprolactone) (PCL-SiOR) single crystals were prepared using a self-seeding method. Silica nanoparticles (40−50 nm) were immobilized onto the surface of single crystals. Subsequent surface-initiated atom transfer radical polymerization (SI-ATRP) of *N*-isopropylacrylamide was carried out on the exposed surface of SiNPs. Dissolution of the polymer single crystal led to Janus nanoparticles with amphiphilic, bicompartment poly(ε-caprolactone) (PCL) and poly(*N*-isopropylacrylamide) (PNIPAM) polymer brushes. The Janus nature of the particle and its detailed characteristics were studied using a variety of techniques including Fourier transform infrared spectroscopy, ^{1}H nuclear magnetic resonance spectroscopy, transmission electron microscopy, and thermogravimetric analysis. These Janus nanoparticles can be readily dispersed in water at room temperature, and because of the lower critical solution temperature (LCST) behavior of PNIPAM brushes in water, Janus nanoparticles exhibit thermo-induced assembly with interesting molecular weight and concentration dependence. Compared with symmetrical PNIPAM-coated SiNPs, Janus particles showed a lower LCST temperature and a much narrower transition range.

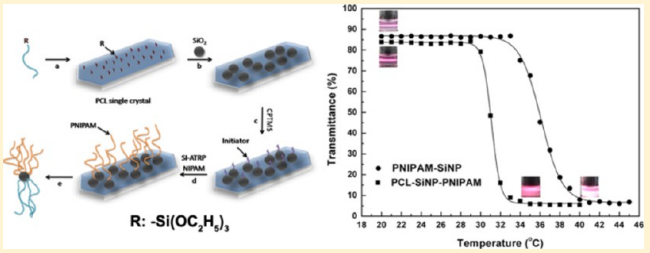

INTRODUCTION

Janus particles, named after the Roman god Janus with two faces toward opposite directions, represent a category of objects possessing a noncentrosymmetric structure, often with a single core that is surrounded by compartmentalized corona.[1−3] Because of their unique structures and extraordinary properties, Janus particles have attracted increasing attention.[4] As a unique type of hybrid materials, Janus particles are promising in the fields such as photonics, sensors, drug delivery, and surfactant.[5−7] They also exhibit unique assembly behavior compared with symmetric particles.[8] Using Janus nanoparticles as the building blocks, much more versatile suprastructure are feasible.[9,10] A variety of assembly structures have been achieved via various mechanisms, such as solvent-triggered interaction,[11,12] electric or magnetic field-induced assembly,[13−16] and ionic strength-induced agglomeration.[17,18] Furthermore, Janus nanoparticles with temperature- or pH- responsive bicompartment polymer brushes showed interesting reversible assembly behavior.[19−21] Among all of these responsive polymers, poly(*N*-isopropylacryamide) (PNIPAM) was the most extensively studied thermoresponsive polymer because of its well-defined lower critical solution temperature (LCST) around 32 °C.[22] Many approaches have been reported for the preparation of Janus particles, including toposelective modification,[23−25] surface nucleation,[26−29] self-assembly of block polymers,[11,30,31] microfluidic technique,[32−34] space-confined assembly,[35,36] electrospinning,[37−39] controlled phase separation,[40−42] and Pickering emulsion-based interfacial synthesis.[43−46] Even though considerable achievements have recently been obtained in this area, developing a facile method to synthesize Janus particles with controlled properties is still a key challenge, especially for Janus nanoparticles with a diameter less than 100 nm.

Morphologically, polymer single crystals often appear as quasi-2D lamellae, which are formed by folding polymer chains back and forth; the chains are perpendicular or oblique to the lamellar surface.[47−49] Given a carefully controlled crystallization condition and chain structure, for end-functionalized polymers, polymer chain ends can be excluded onto the crystal surface. In such cases, these functional groups can then harvest nanoparticles on the polymer single-crystal surface via chemsorption.[47,50,51] Polyethylene oxide (PEO) single crystals have been used as the model system to immobilize nanoparticles in solution.[12,52−58] This method can be referred to as a "polymer single-crystal templating" (PSCryT) approach, and Janus gold nanoparticle consisting of PEO and poly(methyl methacrylate) (PMMA) brushes have been synthesized. Because the functional groups are part of the polymer single-crystal substrate, after coupling reaction the polymer single crystals can be easily dissolved, leading to free Janus nanoparticles. Compared with

Received: September 21, 2012
Revised: October 23, 2012
Published: October 31, 2012

dx.doi.org/10.1021/ma3019987 | *Macromolecules* 2012, 45, 8780−8789

the self-assembled monolayer approach, polymer single crystals have much higher specific surface areas, and the coupling reaction can be carried out in single-crystal suspension, rendering a high yield. The grafting density and molecular weight (MW) of the polymer brushes can also be readily controlled. To better understand polymer−nanoparticle interaction, silica nanoparticles (SiNPs) are most extensively studied because of their low cost, good mechanical property, low toxicity, and well-established surface chemistry and the stable chemical bonding (compared with gold thiol bonds that have been widely used) between the particle and polymer brushes.[59,60] However, very few sub-100 nm Janus nanoparticles have been reported. Among the limited examples, Perro et al.[27] reported a multistep procedure to synthesize ∼80 nm Janus SiNPs using polystyrene nodule as the mask. Zhang et al.[61] reported a Pickering emulsion-based method using 100 nm SiNPs as the surfactant to stabilize styrene/sodium methacrylate aqueous solution emulsion. After the surface-initiated free radical polymerization of both styrene and sodium methacrylate, Janus SiNPs with polystyrene and poly(sodium methacrylate) bicompartment polymer brushes on the opposite surface can be synthesized. Despite these early works, the synthesis of Janus SiNPs with bicompartment polymer brushes is still a challenging research task. Because of the 2D nature and the thinness of the polymer lamellar crystal,the PSCryT approach is particularly useful to prepare sub-100 nm Janus nanoparticles. Herein, following the PSCryT strategy, we demonstrate that end-functionalized hydrophobic polycaprolactone (PCL) can be used as the single-crystal template to immobilize 50 nm SiNPs based on the solid state grafting to mechanism. PNIPAM brushes can then be grafted onto the exposed surface of SiNPs to yield Janus SiNPs with PCL and PNIPAM polymer brushes following the grafting from approach (Scheme 1). The chemical structure, anisotropic morphology, and thermoresponsiveness of Janus nanoparticles have been thoroughly characterized.

EXPERIMENTAL DETAILS

Materials. Hydroxyl-terminated PCL (PCL−OH, M_n 7k g mol^{-1}) was purchased from Polymer Source. *N*-Isopropylacrylamide (NIPAM, 99%) was purchased from Aldrich and recrystallized from hexane three times before use. Colloidal silica in isopropanol (IPA-ST-L, 40−50 nm in diameter, 30−31 wt %) was supplied by Nissan Chemical American. (3-Isocyanatopropyl)triethoxysilane (95%), propylamine (99%+), copper(I) chloride (CuCl, 99.995%+), phosphotungstic acid hydrate (PTA, 95%), ans aluminum oxide (activated, neutral, for column chromatography, 50−200 μm) were purchased from Aldrich and used as received. (*p*-Chloromethyl)phenyltrimethoxysilane (95%) was purchased from Gelest and used without further purification. Rutheniumtetraoxide (RuO_4, 99.5%+) and sodium periodate (99%+) were purchased from Structure Probe and used as received.

Synthesis of Janus Silica Nanoparticles. Janus SiNPs are denoted as *A-SiNP-B*. A and B stand for the ligand/polymer brushes grafted on SiNPs.

Synthesis of Alkoxysilane-Terminated PCL (PCL-SiOR). We dissolved 300 mg PCL−OH (0.043 mmol) in 10 mL of anhydrous dichloromethane in a flask under nitrogen protection with continuous magnetic stirring. One mL of (3-isocyanatopropyl)triethoxysilane (4.0 mmol) was then added dropwise to the PCL solution. After 12 h, the reaction was stopped, and the solution was concentrated using a rotary evaporator. Precipitating the concentrated solution in methanol yielded PCL-SiOR white powder, which was washed thoroughly with methanol and dried in vacuum at room temperature for 24 h before use.

Growth of PCL-SiOR Single Crystals. PCL-SiOR (3.0 mg) was added into 1-butanol (10.0 g) and was heated to 60 °C for 10 min until the polymer was completely dissolved. The solution was quenched to −10 °C for 2 h and then brought to 45 °C for 10 min to form crystal seeds. Solution crystallization was then conducted at room temperature for 24 h. The resultant single crystals were collected through centrifugation to remove uncrystallized polymers and were redispersed in 3 g 1-butanol for the following immobilization process.

Synthesis of PCL- and Initiator-Modified Janus SiNPs (PCL-SiNP-I). The PCL-SiOR single-crystal suspension in 1-butanol was mixed with colloidal silica solution in isopropanol. The mass ratio between the crystal suspension and nanoparticle solution was 3/1. A small amount of deionized water (0.25 wt %) was added to the mixture as the catalyst. The immobilization process was conducted for 24 h at room temperature. Free particles were then removed through centrifugation.

An isopropanol suspension (20 mL) of PCL-SiOR single crystal covered with SiNPs (78 mg PCL-SiOR) was poured in a flask with a magnetic stir bar. After the flask was sealed, 0.4 mL of propylamine was added to the flask, followed by dropwise addition of 0.4 mL of (*p*-chloromethyl)phenyltrimethoxysilane. The mixture was stirred at room temperature overnight. After completion of reaction, a multiple centrifugation process was used to remove the free initiator. The single-crystal/SiNPs hybrid with bare SiNP surface attached with initiator was then redispersed in isopropanol for the following surface-initiated polymerization. To verify the successful attachment of initiators on the nanoparticle surface, we dissolved these SiNP-decorated single crystals in acetone to yield Janus PCL-SiNP-I. PCL-SiNP-I was collected and purified through multiple centrifugations. The particles were dried in a vacuum oven at room temperature for 24 h before characterizations.

Synthesis of PCL- and PNIPAM-modified Janus SiNPs (PCL-SiNP-PNIPAM) via Surface-Initiated Atom Transfer Radical Polymerization (SI-ATRP). Tri(2-dimethylaminoethyl)amine (Me_6TREN) was prepared as reported.[62] Typically, CuCl (4.75 mg, 0.048 mmol) single crystal decorated with SiNPs and the initiator (from 39 mg PCL-SiOR) were dispersed in 4.5 g isopropanol, and NIPAM (0.45 g, 4 mmol) and (*p*-chloromethyl)phenyltrimethoxysilane (4.4 μL, 0.02 mmol) were added in a Schlenk tube under nitrogen. Three cycles of freeze−pump−thaw were conducted to remove air in the tube. Me_6TREN (11.04 mg, 0.048 mmol) was then added to the tube in frozen state, followed by two additional freeze−pump−thaw cycles. During the thawing period, the reaction reagents were mixed using a magnetic stir bar under nitrogen. The polymerization was conducted at 35 °C under vacuum. After 48 h, the polymerization was stopped by opening the tube to air. The reaction mixture was centrifuged, and the

Scheme 1. Schematic Illustration of the Synthesis Procedure of Janus Silica Nanoparticles (a) and the Side-View of a PCL (M_n ≈ 7k g/mol) Single Crystal Showing the Chain Folding (b)

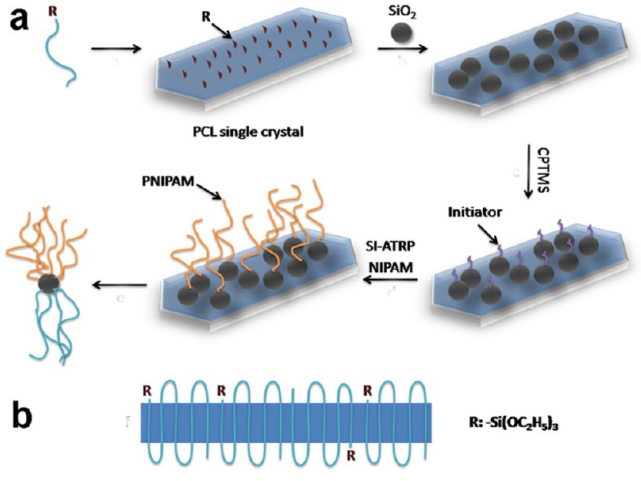

dx.doi.org/10.1021/ma3019987 | Macromolecules 2012, 45, 8780−8789

isolated PCL single crystals decorated with SiNPs were obtained. The supernatants were purified using aluminum oxide column chromatography three times to remove copper salt, followed by precipitation in diethyl ether to form "free" PNIPAM, which was collected by filtration, washed thoroughly with diethyl ether, and dried in vacuum at room temperature for at least 24 h before further characterization. PCL-SiNP-PNIPAM was collected by multiple centrifugations, followed by dissolution of the single crystal in acetone. The Janus nanoparticles were dried in vacuum at room temperature for 24 h before further studies.

Synthesis of Symmetrically Modified Silica Nanoparticles. *Synthesis of Initiator-Modified SiNPs.* Colloidal silica in isopropanol (1 g) was diluted using isopropanol (15 mL). Propylamine (0.3 mL) was then added to the solution, followed by dropwise addition of (*p*-chloromethyl)phenyltrimethoxysilane (0.3 mL). The mixture was sealed and then stirred overnight using a magnetic stir bar at room temperature. After completion of the reaction, the initiator-functionalized SiNPs (I-SiNP) were collected using centrifugation and thoroughly washed with isopropanol to remove the free initiator. The particles were then dried in vacuum at room temperature for 24 h before further reaction.

Synthesis of PNIPAM-Modified Symmetric SiNPs (PNIPAM-SiNP) via SI-ATRP. CuCl (4.66 mg, 0.047 mmol), I-SiNP (60 mg), NIPAM (0.44 g, 3.9 mmol), and (*p*-chloromethyl)phenyltrimethoxysilane (4.4 μL, 0.02 mmol) were added to a Schlenk tube under the protection of nitrogen. Three cycles of freeze−pump−thaw were then conducted to remove air in the tube. Me_6TREN (10.81 mg, 0.047 mmol) was then added to the tube in the frozen state, followed by two additional freeze−pump−thaw cycles. During the period of thawing, the reaction reagents were mixed using a magnetic stir bar under nitrogen. The polymerization was conducted at 35 °C under vacuum. After 24 h, the polymerization was stopped by opening the tube to air. SiNPs uniformly grafted with PNIPAM (PNIPAM-SiNP) were obtained and purified via a multiple centrifugation process. The supernatant of each centrifugation cycle was collected, passed through aluminum oxide column three times, and precipitated in diethyl ether to yield free PNIPAM. Finally, both particles and the free polymer were dried in vacuum at room temperature for 24 h before characterization.

Cleavage of PNIPAM Chains from SiNP Surface. To verify that during SI-ATRP free polymer obtained from sacrificial initiator has similar MW and polydispersity (PDI) with polymer brushes grafted on the particle surface, PNIPAM brushes were cleaved from PNIPAM-SiNP for GPC measurement to compare with free PNIPAM. The detailed procedure is described as follows. 50 mg PNIPAM-SiNP was dispersed in 5 mL of deionized water in a plastic vial. In the dispersion, 200 μL of hydrofluoric acid (48 wt %) was added under magnetic stirring. The reaction was conducted at room temperature for 4 h. The solution was then dialyzed against deionized water for 3 days to remove small molecules. After the purification, the polymer solution was dried in vacuum oven at 60 °C for 48 h before GPC measurements.

Characterization. ^{1}H nuclear magnetic resonance (NMR) spectra were recorded on a Varian 300 MHz spectrometer using $CDCl_3$ as the solvent and tetramethylsilane (TMS) as the internal standard. Infrared spectra were recorded using a Digilab, UMA 600 Fourier transform infrared (FTIR) spectroscopy spectrometer with KBr pellets in the transmission mode. For the preparation of an FTIR specimen, 1 g sample solution (0.1 wt %) was drop cast on the surface of KBr pellets and dried under vacuum for 24 h. Before FTIR test, the KBr pellets were dried again using infrared lamp for at least 10 min. Transmission electron microscopy (TEM) experiments were carried out using a JEM2100 TEM operated at an acceleration voltage of 200 kV. One drop (5 μL) of diluted sample suspension (crystal or nanoparticles) was drop cast on a carbon-coated nickel TEM grid. A piece of filter paper was used to quickly blot the grid and minimize particle aggregation. Some TEM samples were stained by either RuO_4 vapor or PTA aqueous solution and will be noted in the discussion as needed. Scanning electron microscopy (SEM) experiments were conducted using a Zeiss Supra 50VPSEM with an acceleration voltage of 10 kV. SEM samples were prepared by depositing nanoparticle suspensions onto the surface of a precleaned glass slide. To increase conductivity, we coated samples with platinum (25 s, 40 mA) by a Cressington sputter coater 208HR before observation. Gel permeation chromatography (GPC) tests were carried out using a Waters GPC with a 1525 binary HPLC pump and a Waters 2414 refractive index detector. All GPC samples were conducted using tetrahydrofuran as the carrier solvent with a flow rate of 1.0 mL/min at room temperature (~25 °C). Standard monodispersed polystyrenes (Shodex standard, Kawasaki, Japan) were used for calibration. Thermogravimetric analysis (TGA) was performed using a Perkin-Elmer TGA 7. The samples were heated from 30 to 900 °C under an air atmosphere with a heating rate of 5 °C/min. Optical transmittance of aqueous solutions of both Janus and symmetric nanoparticles solutions were acquired at a wavelength of 800 nm on an Ocean Optics USB4000 miniature Fiber Optic Spectrometer using a thermostatically controlled cuvette.

RESULTS AND DISCUSSION

SiNPs with a Single PCL Patch. Janus SiNPs with a single PCL patch on the surface were successfully synthesized via a PSCryT method using PCL-SiOR single crystals as the substrate, followed by subsequent dissolution of the single crystal. In the first step, PCL−OH was functionalized using organic silane-bearing isocyanate to introduce −SiOR at the PCL chain end. During the self-seeding crystallization process, −SiOR groups were excluded onto the lamellar surface. This thin PCL-SiOR lamellar crystal mimics nanoscale "tape" and can be utilized for chemisorption of SiNPs (Scheme 1). Figure 1 shows TEM images of PCL-SiOR single crystals before and

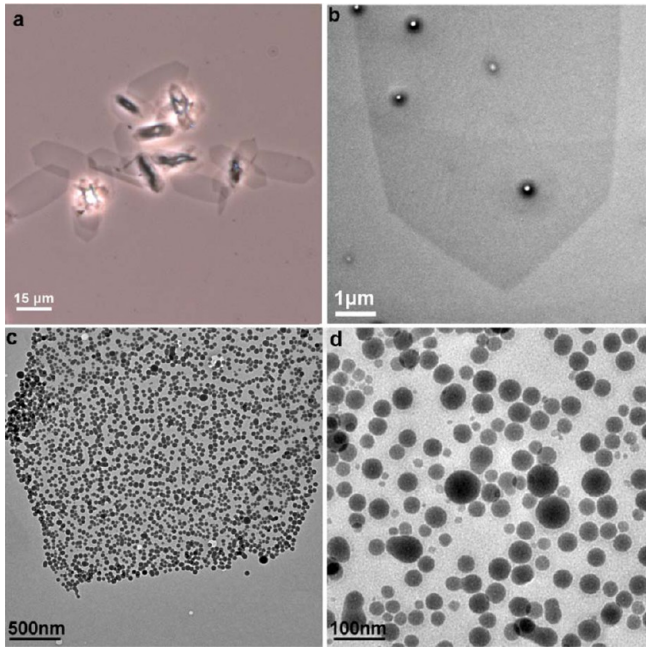

Figure 1. (a) Phase-contrast optical microscopy image of PCL-SiOR single crystals. (b) Transmission electron microscopy (TEM) image of PCL-SiOR single crystal. (c,d) PCL-SiOR single crystal immobilized with silica nanoparticles (40−50 nm) under different magnifications.

after being immobilized with SiNPs. Using the self-seeding method, hexagonal 2D lamellae crystals can be formed from the dilute solution of PCL in 1-butanol, as shown in Figure 1a,b. Subsequent PSCryT adsorption of SiNPs (Scheme 1) can then be conducted by simply mixing the single-crystal suspension and SiNPs solution under gentle stirring. The TEM images (Figures 1c,d) show that due to the covalent bonding between the −SiOR groups and SiNPs the latter can be exclusively

dx.doi.org/10.1021/ma3019987 | Macromolecules 2012, 45, 8780−8789

immobilized onto the crystal surface to form a uniform 2D nanoparticle sheet. After the crystals were dissolved in acetone, SiNPs with a single PCL path could be obtained. ^{1}H NMR (Figure 2a) and FTIR spectra (Figure 3) were used to confirm

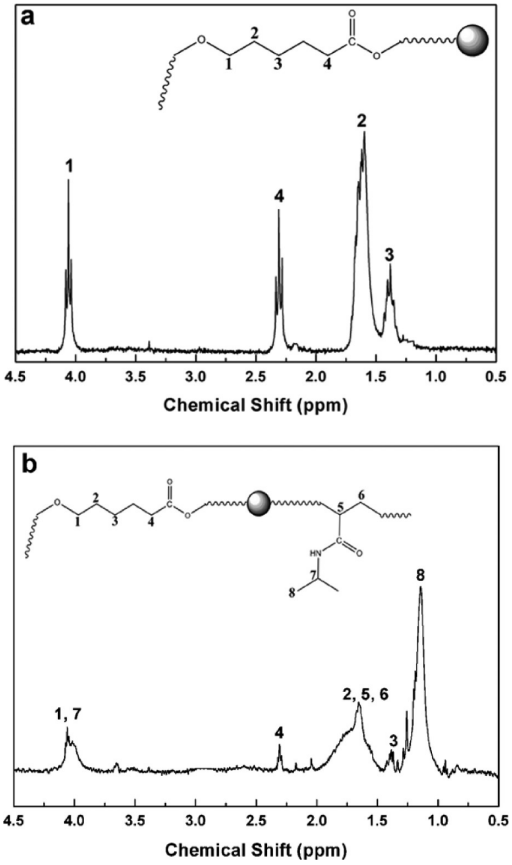

Figure 2. ^{1}H Nuclear magnetic resonance (NMR) spectrum of PCL-SiNP (a) and PCL-SiNP-PNIPAM (b) Janus nanoparticles.

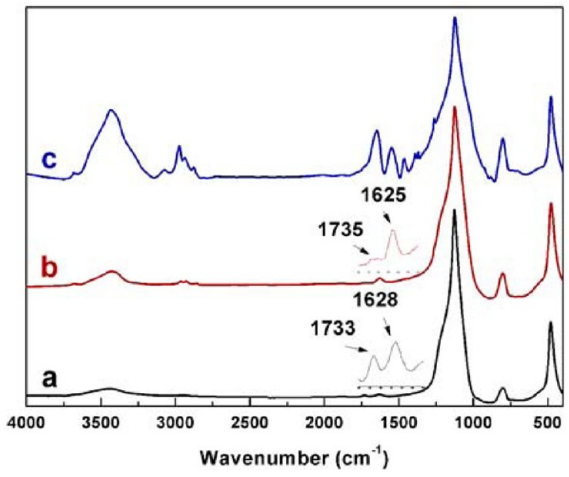

Figure 3. Fourier transform infrared spectroscopy (FTIR) spectrum of PCL-SiNP (a), PCL-SiNP-I (b), and PCL-SiNP-PNIPAM (c).

the successful attachment of PCL polymer brushes on SiNPs. A typical NMR spectrum of PCL macromolecules can be observed in Figure 2a with intensive peaks at δ ~4.1, 2.3, 1.6, and 1.4. The peak positions and integral areas agree with the NMR spectrum of pure PCL; however, comparing NMR peaks of immobilized PCL with free PCL, the peak width was broadened. This is because the motion of the polymer chains was restricted by tethering one chain end to the solid surface.[63] In the FTIR spectra of PCL-coated SiNP, the band at 1733 cm^{-1} was ascribed to C═O stretching in the PCL moiety. Because of the small amount of PCL grafted on SiNPs (~10 wt % according to TGA, see later discussion), these FTIR bands were weak compared with bands at 1100 (Si−O stretching), 500 (Si−O bending), and 800 cm^{-1} (Si−O−Si bending). The 1628 cm^{-1} band was attributed to the overtone of silica.[64]

Janus Nanoparticles with Bicompartment Brushes via "Grafting-From" Method. After SiNPs have been successfully immobilized onto single-crystal surface, SI-ATRP was adopted to grow hydrophilic PNIPAM brushes on the bare surface of the SiNPs. To this end, the bare surface of the SiNPs on PCL single crystals was first functionalized with (*p*-chloromethyl)phenyltrimethoxysilane, which was used to initiate ATRP of NIPAM following the procedure discussed in the Experimental Details. Attachment of the initiator molecules was confirmed by FTIR (Figure 3). In the FTIR spectra of PCL-SiNP-I Janus particles, because of additional alkyl groups introduced by grafting of initiators, bands at ~2900 cm^{-1}, which are due to the stretching of C−H groups, are strengthened. Furthermore, relative intensity of the bands at 1625 and 1735 cm^{-1} dramatically increased compared with that of PCL-coated SiNP, which can be attributed to the vibration of benzene ring structure in initiator moieties that strengthened the absorption at 1625 cm^{-1}.

SI-ATRP was subsequently conducted from the I-SiNPs on the PCL-SiOR single crystals. To better control the polymerization, free (*p*-chloromethyl)phenyltrimethoxysilane was added to the polymerization media as the sacrificial initiator. Polymerization proceeded in isopropanol for 48 h using Me_6TREN/CuCl as the catalyst complex at 35 °C. After completion of polymerization, the single-crystal/SiNPs hybrids were thoroughly washed with isopropanol, and the supernatant was precipitated into ethyl ether to yield free PNIPAM polymer for molecular-weight analysis. Figure 4 shows TEM images of PCL single crystals coated with SiNPs and PNIPAM. Single-crystal morphology retained after the polymerization process, and SiNPs are bonded with the crystal. As illustrated in Figure 4b, although the contrast is weak without staining, it appears that SiNPs are covered with polymer coating. To confirm that

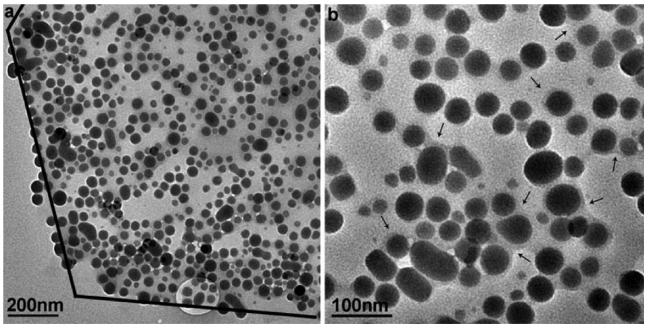

Figure 4. Transmission electron microscopy (TEM) images of PCL-SiOR single crystals immobilized with silica nanoparticles after surface-initiated ATRP under different magnifications. The solid lines in panel a indicate the edges of polymer single crystal. Note the polymer coating indicated by arrows on b compared with the TEM image of PCL single crystal immobilized with silica nanoparticles before ATRP (Figure 1).

dx.doi.org/10.1021/ma3019987 | *Macromolecules* 2012, 45, 8780−8789

PNIPAM was successfully grafted on SiNPs, the single crystal was dissolved in acetone, and the resultant Janus PCL-SiNP-PNIPAM was collected for NMR and FTIR studies. The NMR spectrum of PCL-SiNP-PNIPAM is shown in Figure 2b. On the basis of the integral areas of two peaks with chemical shifts at δ ~2.3 and ~1.1 in Figure 2b, we can calculate that the molar ratio between repeating units of PCL and PNIPAM brushes is approximately 1:3. From the FTIR spectrum of PCL-SiNP-PNIPAM, we can clearly observe the two strong bands attributed to amide I (1654 cm^{-1}, C═O stretching) and amide II (1549 cm^{-1}, N−H stretching) from PNIPAM brushes.

The Janus nature of PCL-SiNP-PNIPAM was demonstrated using TEM with different staining methods. Figure 5 shows the TEM images of PCL-SiNP-PNIPAM without staining and of those stained with RuO_4 and PTA, respectively. Without staining, SiNPs can be seen, whereas the polymer shell is not clear, as shown in Figure 5a,b. After staining with RuO_4, the asymmetric structure can be clearly demonstrated, as shown in Figure 5c,d. Because RuO_4 selectively stains PCL patch, we can clearly see the PCL patch of ~5−30 nm in size, occupying approximately 1/6 of the projected SiNP surface area. Note that the size of the patch is strongly dependent on the orientation of the particle with respect to the electron beam. Figure 5e,f shows the TEM images of PCL-SiNP-PNIPAM after dropcasting from an acetone solution followed by PTA staining. In this case, grayish PCL patches were observed, whereas a thin layer of PNIPAM brushes, which was also negatively stained by PTA solution, can also be seen covering the surface of SiNPs. Note that the unclear interface between PCL and PNIPAM brushes in Figure 5f is due to the orientation of SiNPs. A control experiment using aqueous solution of PCL-SiNP-PNIPAM Janus nanoparticles for TEM imaging was also conducted to illustrate further the structure of Janus nanoparticles, and the results are shown in the inset of Figure 5f. Only core−shell-like structure was observed. and the asymmetric feature previously observed was completely absent. Tilting experiments of the TEM grid holder were conducted to eliminate the effects from the orientation of nanoparticles; no obvious differences were observed. This "apparent" symmetric staining of the Janus particle is because the hydrophobic PCL brushes collapse in aqueous solution while PNIPAM brushes are in a swollen state. (See the later discussion for a detailed description of the behavior of polymer brushes in aqueous solution.) PNIPAM occupies the major part of the SiNPs and covers the PCL patch in the aqueous condition. Negative staining using PTA therefore can show only the "apparent" symmetric PNIPAM patches. On the basis of the above TEM experiments, the Janus structure of PCL-SiNP-PNIPAM nanoparticles composed of bicompartment polymer brushes with amphiphilic nature was successfully demonstrated.

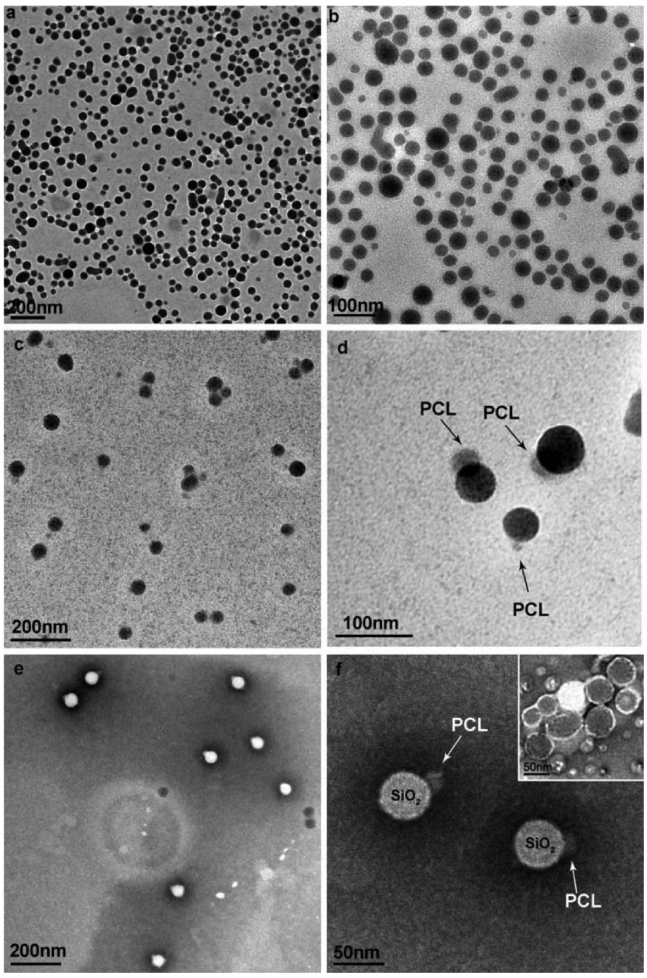

Figure 5. Transmission electron microscopy (TEM) images of PCL-SiNP-PNIPAM Janus nanoparticles with different staining methods: (a,b) without staining before observation, (c,d) stained with RuO_4 for 30 min before observation, and (e,f) solution cast from an acetone solution and stained with PTA aqueous solution (2 wt %) for 1 min before observation. The inset in panel f shows the TEM image of PCL-SiNP-PNIPAM solution cast from aqueous solution at room temperature and stained with PTA aqueous solution (0.2 wt %) for 1 min.

The MW and PDI of PNIPAM brushes on Janus particles were obtained using GPC. Figure 6a shows the GPC traces of PNIPAM polymerized from sacrificial initiators in the PCL-SiNP-PNIPAM synthesis. Because of the "living" nature of ATRP, the as-synthesized polymer molecules had relatively narrow PDI of ~1.2.[53] It has also been widely accepted that the grafted polymer on substrates in SI-ATRP has similar MW and PDI compared with free polymers initiated from sacrificial initiator.[65] This was also confirmed in our case using symmetric PNIPAM-SiNP as the model system. As shown in Figure 6b, the MW and PDI of free PNIPAM and cleaved PNIPAM are very close to each other. Therefore, we can conclude that the number-average MW (M_n) of PNIPAM brushes on PCL-SiNP-PNIPAM and PNIPAM-SiNP symmetric nanoparticles is 6500 and 7400 g mol^{-1}, respectively. These data are summarized in Table 1and will be used for the grafting density calculation.

Grafting Density of Polymer Brushes on Janus and Symmetric SiNPs. In PCL-SiOR lamellar crystals, PCL-SiOR chains are perpendicular to the crystal surface, and they fold back and forth. To estimate the number of grafted PCL chains on SiNPs, we need a number of folds per polymer chain. To this end, AFM was used to estimate the overall thickness of the crystal, which, in combination with the polymer M_n, can lead to an estimation of the number of folds. Figure 7 shows an AFM image of a PCL-SiOR single crystal and a height scanning profile of the crystal (lower left inset), indicating that the overall thickness of the crystal is ~10 nm. Combining the thickness of single-crystal lamellae, PCL M_n, and crystal structure,[66] we can calculate that a single PCL-SiOR chain folds ~4.3 times along the direction perpendicular to the lamellar surface (Scheme 1b). Because of their large size, we assume that all −SiOR end groups are excluded on the crystal

dx.doi.org/10.1021/ma3019987 | Macromolecules 2012, 45, 8780−8789

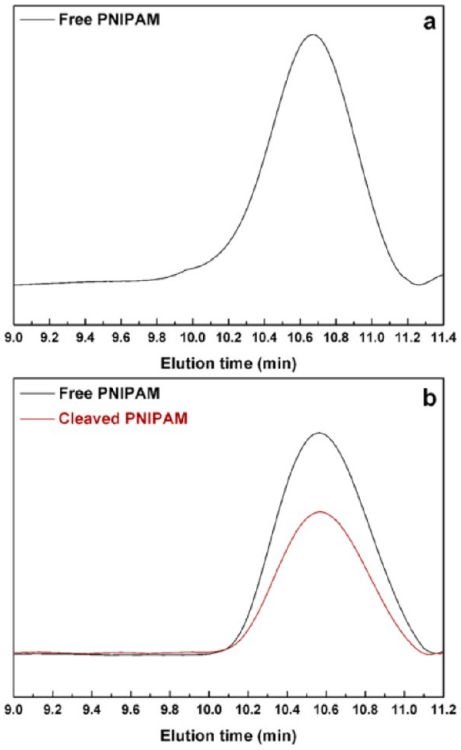

Figure 6. Gel permeation chromatography (GPC) curves of: (a) free PNIPAM from PCL-SiNP-PNIPAM Janus nanoparticles and (b) free PNIPAM from PNIPAM-SiNP symmetric nanoparticles and PNIPAM cleaved from symmetric nanoparticles.

surface. The areal density of alkoxysilane groups on the PCL crystal surface could then be estimated to be 1.07/nm^2. If we use the 2D projection of SiNPs on crystal lamellae as the grafted area, then the estimated number of PCL chains is 1946 per particle. However, this number can serve only as a theoretical upper-limit because during the calculation, the grafted area was overestimated.

To obtain more accurate numbers of grafted chains for both PCL and PNIPAM brushes, we obtained TGA curves of different SiNPs, as shown in Figure 8. From the residual weight percentage at 900 °C of each curve, assuming that the SiNPs have a spherical shape, the mean diameter of SiNPs is 45 nm, and the density is 2.07 g/cm^3, we can calculate that ~943 PCL chains (7k g/mol) were grafted on one SiNP, forming the PCL compartment, whereas 2729 PNIPAM chains occupy the rest of the surface area and form the PNIPAM compartment. Using the chain number of both PCL and PNIPAM on the Janus PCL-SiNP-PNIPAM, the molar ratio between the repeating units of them was calculated to be ~1:2.8, which is consistent with the NMR result. (See the previous discussion.) On the basis of the TGA result, the number of initiator molecules grafted on one PCL-SiNP-I Janus particles can also be

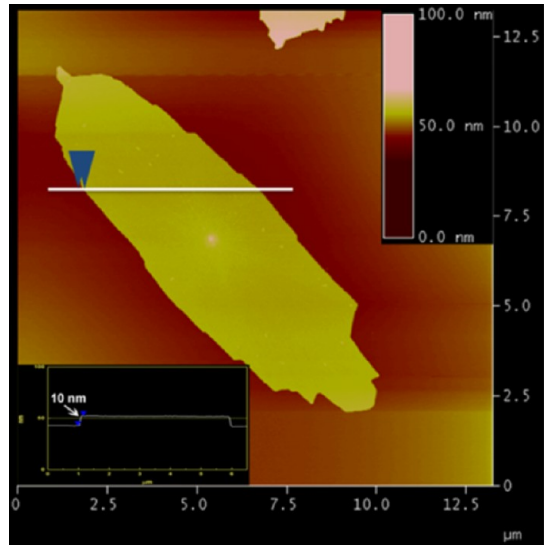

Figure 7. Atomic force microscopy (AFM) images of a 7 kg/mol PCL-SiOR single crystal prepared in this study and the corresponding height profile (inset).

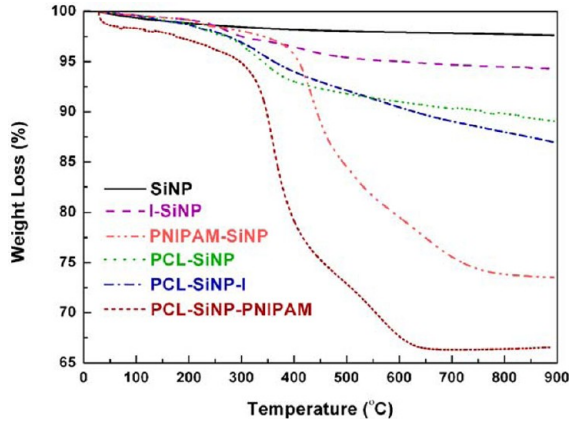

Figure 8. Thermogravimetry analysis (TGA) curves of bare silica nanoparticles, symmetric silica nanoparticles, and Janus silica nanoparticles with different patches.

estimated to be ~16 713, which indicated that ~16% of the anchored initiator successfully initiated the SI-ATRP process. The average grafting density of PCL and PNIPAM polymer brushes on SiNP was 0.58/nm^2, which is comparable to our previous studies on Janus gold nanoparticles with bicompartment polymer brushes.[52,53]

Thermoresponsive Behavior of PCL-SiNP-PNIPAM Janus Nanoparticles. First, to understand the influence of anisotropy of Janus nanoparticles on the LCST behavior, a comparison was made between the Janus nanoparticles solution and symmetric nanoparticles solution. Turbidity of the Janus

Table 1. Characterization of Polymer Brushes on PCL-SiNP-PNIPAM Janus Nanoparticles and PNIPAM-SiNP Symmetric Nanoparticles

	M_n^{PCL}	M_n^{PNIPAM} (free)[a]	M_n^{PNIPAM} (grafted)[a]	PDI[b]	n_{PCL}[c]	n_{PNIPAM}[c]	σ[d]
PCL-SiNP-PNIPAM	7000	6500		1.18	943	2729	0.58
PNIPAM-SiNP		7200	7400	1.19		2241	0.36

[a]Number-average molecular weight of corresponding polymer from GPC (g/mol). [b]Polydispersity of PNIPAM obtained using GPC. [c]Number of polymer chains on one silica nanoparticle. [d]Grafting density (chains/nm^2).

dx.doi.org/10.1021/ma3019987 | Macromolecules 2012, 45, 8780−8789

PCL-SiNP-PNIPAM and symmetric PNIPAM-SiNP nanoparticle aqueous solution (0.1 wt %) was measured by monitoring the temperature-dependence optical transmittance at 800 nm. As shown in Figure 9, at low temperature, both

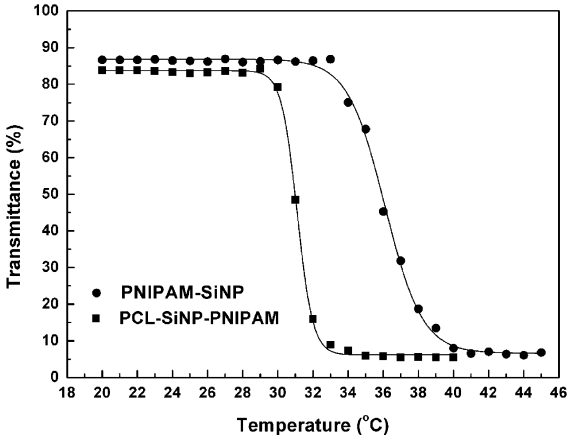

Figure 9. Temperature-dependent optical transmittance at 800 nm obtained from aqueous solutions of PCL-SiNP-PNIPAM and PNIPAM-SiNP nanoparticles (0.1 wt %).

solutions were relatively transparent, and the transmittance decreased dramatically at LCST regions of PNIPAM. The transition for Janus particle is much sharper, and the temperature ranges of Janus and symmetric nanoparticles are about 31−34 and 34−43 °C, respectively. Janus nanoparticle transition also occurred ∼4 °C lower. Wu et al.[67] recently reported a systematic study on the preparation of SiNPs with uniformly coated PNIPAM brushes and their thermoresponsive properties. By utilizing dynamic light scattering and optical transmittance characterizations of nanoparticle solution in water, they found that the thermal phase transition of PNIPAM brushes on the SiNPs surface happened within a wide temperature range from 33 to 47 °C, which is similar to our symmetric SiNP results.

For symmetric PNIPAM-SiNPs, upon reaching LCST, PNIPAM chains go through a coil−globule transition, which leads to nanoparticle agglomeration. For Janus nanoparticles with one patch composed of PNIPAM brushes, it has been found that the property of the other patch would greatly influence the thermoresponsive behavior.[21,68] In our study, because M_n, PDI, and grafting density of polymer brushes on both Janus and symmetric nanoparticles are similar, the faster transition and lower transition temperatures of Janus nanoparticles are ascribed to the effect of the PCL hydrophobic patch on Janus particle. As shown in Scheme 2, for a Janus PCL-SiNP-PNIPAM, when the temperature is lower than LCST of PNIPAM brushes because the relatively large surface area of the Janus nanoparticle was covered by the hydrophilic polymer brushes, PCL patch would collapse and be covered by surrounding PNIPAM brushes, as evidenced by the TEM image shown in the inset of Figure 5f. As the temperature approaches LCST, the PNIPAM chain itself starts to go through a coil−globule transition and eventually would not be able to cover the collapsed PCL patch on the Janus nanoparticles. Under this condition, exposed hydrophobic PCL patches in water would induce the agglomeration of nanoparticles and lower the transparency of aqueous dispersion. When the temperature further increases, PNIPAM brushes would continue to collapse,

Scheme 2. Schematic Illustration of the Proposed Lower Critical Solution Temperature (LCST) Behavior of PCL-SiNP-PNIPAM Janus Particles in Aqueous Solution[a]

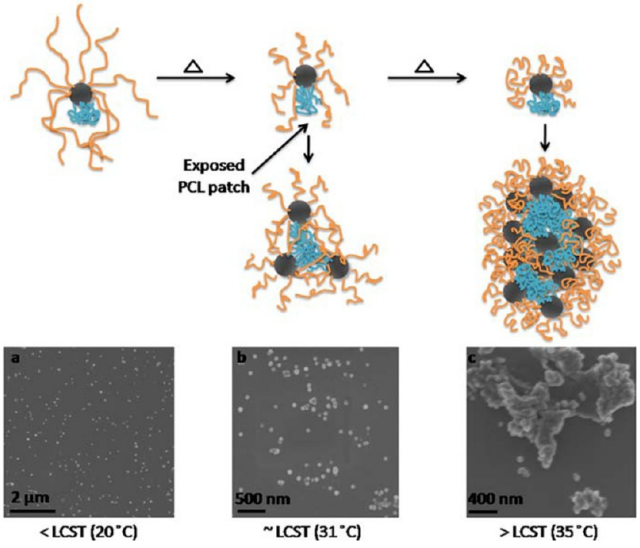

[a](a−c) at the bottom show scanning electron microscopy (SEM) images of the assembled structures of Janus nanoparticles in solution at corresponding temperatures.

and eventually not only the PCL patch would completely be exposed to aqueous phase but also the PNIPAM corona would become "sticky" and start to contribute to the formation of agglomerate. Apparently, in the case of symmetric SiNPs with PNIPAM brushes, no extra hydrophobic interaction can be introduced upon increasing temperature, and PNIPAM brushes can still maintain relatively good water solubility in the early stage of transition; higher transition temperature and wider transition range has thus been observed.

Molecular Weight and Concentration Effects of the Thermoresponsive Behavior. To evaluate further the thermal-transition behavior of Janus nanoparticles synthesized in this study, we synthesized and studied two more PCL-SiNP-PNIPAM samples with different MW of PNIPAM. For the convenience of discussion in this section, the Janus nanoparticles are denoted as PCL-SiNP-PNIPAM$_A$, where A represents M_n of PNIPAM brushes of each sample obtained by GPC. By measuring the turbidity of three nanoparticle solutions with various concentrations using the same method previously described, the MW dependence and concentration dependence of the LCST behavior of PCL-SiNP-PNIPAM Janus nanoparticles can be established.

To eliminate the grafting density effects of PNIPAM brushes on the LCST behavior of nanoparticles, it is necessary to characterize thoroughly all three Janus nanoparticle samples to ensure that the polymer brushes have similar grafting densities. Figure 10 shows the detailed GPC, NMR, and TGA results of three Janus nanoparticles synthesized in this study. From the GPC curves it can be found that the M_n values of the PNIPAM brushes grafted on the three Janus nanoparticles are 4700, 6500, and 9800 g/mol, respectively. The NMR spectrum shown in Figure 10b indicated that the molar ratios between the repeating units of PCL and PNIPAM brushes on Janus nanoparticles are 1:2, 1:3, and 1:4.5 for PCL-SiNP-PNIPAM$_{4.7k}$, PCL-SiNP-PNIPAM$_{6.5k}$, and PCL-SiNP-PNIPAM$_{9.8k}$, respectively. By combining with the TGA data

dx.doi.org/10.1021/ma3019987 | Macromolecules 2012, 45, 8780−8789

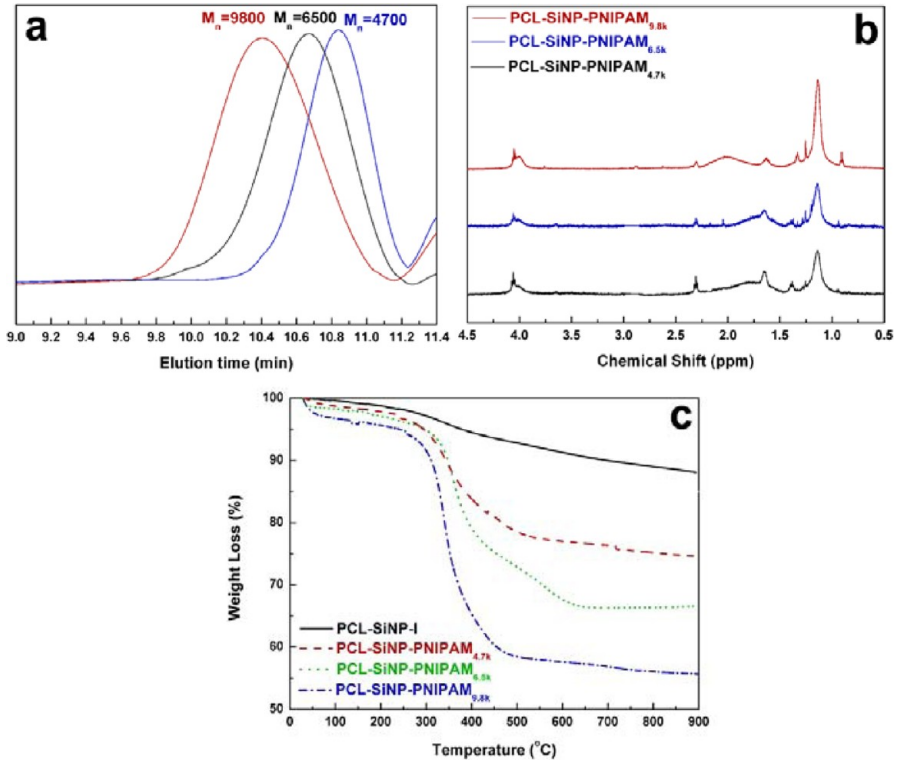

Figure 10. (a) Gel permeation chromatography curves of free PNIPAM obtained from three PCL-SiNP-PNIPAM nanoparticles. (b) ^{1}H nuclear magnetic resonance spectrum of PCL-SiNP-PNIPAM$_{4.7k}$, PCL-SiNP-PNIPAM$_{6.5k}$, and PCL-SiNP-PNIPAM$_{9.8k}$ nanoparticles in chloroform-*d*. (c) Thermogravimetry analysis of PCL-SiNP-I Janus nanoparticles and Janus nanoparticles with different molecular weights of PNIPAM brushes.

Table 2. Characterizations of Polymer Brushes on Janus Nanoparticles with Different PNIPAM Molecular Weight

	M_n^{PCL} (g/mol)	M_n^{PNIPAM} (g/mol)[a]	PDI_{PNIPAM}[b]	n_{PCL}[c]	n_{PNIPAM}[c]	σ[d]
PCL-SiNP-PNIPAM$_{4.7k}$	7000	4700	1.13	943	2128	0.48
PCL-SiNP-PNIPAM$_{6.5k}$	7000	6500	1.18	943	2729	0.58
PCL-SiNP-PNIPAM$_{9.8k}$	7000	9800	1.23	943	2584	0.55

[a]Number-average molecular weight of free PNIPAM obtained using GPC. [b]Polydispersity of free PNIPAM obtained using GPC. [c]Number of polymer brushes grafted on the surface of one silica nanoparticle. [d]Grafting density of polymer brushes (chains/nm^2)

shown in Figure 10c, similar grafting density of polymer brushes on SiNP surface can be calculated for all three samples. These data are summarized in Table 2.

The MW dependence of the LCST behavior of PCL-SiNP-PNIPAM Janus nanoparticles is shown in Figure 11. It can be noted that with longer PNIPAM chain on the surface, the onset of LCST upshifts (29 °C for PCL-SiNP-PNIPAM$_{4.7k}$, 31 °C for PCL-SiNP-PNIPAM$_{6.5k}$, and 33 °C for PCL-SiNP-PNIPAM$_{9.8k}$), whereas the temperatures at which all samples reached lowest transmittance are relatively constant. This phenomenon can be explained using the mechanism proposed in a previous discussion. Because the initial decrease in the transmittance of nanoparticle solution was induced by the hydrophobic interaction between PCL patches between different particles, with a constant PCL domain size, PNIPAM brushes with higher MW would require higher temperature to collapse to a certain extend when the PCL domain is exposed to the aqueous environment to trigger the LCST.

The LCST behavior of Janus nanoparticles is also concentration-dependent. Figure 12 shows the temperature-dependent transmittance of Janus nanoparticle solutions with different PNIPAM MWs and particle concentrations. As depicted in the transmittance curves, for all three Janus particle samples, the thermal-transition broadens as the particle

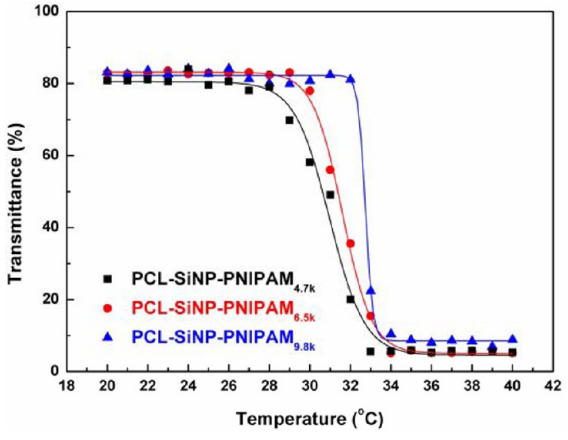

Figure 11. Temperature-dependent optical transmittance at 800 nm obtained from aqueous solutions of PCL-SiNP-PNIPAM nanoparticles with different PNIPAM molecular weights at a constant concentration (0.1 wt %).

concentration decreases, which can be attributed to the lower possibility for nanoparticles to aggregate with each other under diluted condition. However, the onset transition temperatures

dx.doi.org/10.1021/ma3019987 | *Macromolecules* 2012, 45, 8780−8789

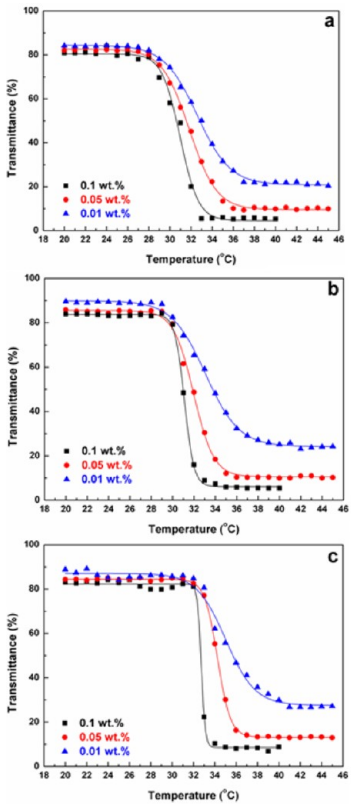

Figure 12. Temperature-dependent optical transmittance at 800 nm obtained from aqueous solutions of PCL-SiNP-PNIPAM nanoparticles with different PNIPAM molecular weight at different concentration (0.1, 0.05, and 0.01 wt %): (a) PCL-SiNP-PNIPAM$_{4.7k}$, (b) PCL-SiNP-PNIPAM$_{6.5k}$, and (c) PCL-SiNP-PNIPAM$_{9.8k}$.

at different concentrations are relatively constant. This observation further confirmed the mechanism previously proposed: LCST is triggered by the polymer brush collapsing on individual particles, which is less affected by the particle concentration. Even though the possibility of collision between nanoparticles is decreased due to lowered solution concentration, the decreased transmittance at the specific temperature still evidenced the collapse of PNIPAM chain, which resulted in hydrophobic interaction between PCL domains.

CONCLUSIONS

In this study, a simple and versatile approach of synthesizing Janus SiNPs with amphiphilic properties was demonstrated using the PSCryT method. PCL single crystals with alkoxysilane groups distributed on the surface were utilized as a solid-state substrate for immobilization of SiNPs. The exposed bare surface of SiNPs was further functionalized using organosilane bearing halogen group, followed by SI-ATRP of NIPAM. Through this two-step process, amphiphilic Janus SiNPs with hydrophobic (PCL) and hydrophilic (PNIPAM) patches were successfully synthesized, and the asymmetric nature was demonstrated by TEM using different staining methods. These Janus particles can be readily dispersed in water to form uniform and transparent suspension at room temperature, and the PNIPAM brushes on the surface can trigger thermoresponsive assembly of the Janus nanoparticles. Compared with SiNPs with uniformly grafted PNIPAM brushes, Janus particles in our study showed a lower thermal transition temperature and much narrower transition range. This unique behavior was attributed to the presence of PCL patch on the surface of Janus particles: hydrophobic interaction between these patches on different particles provides much greater driving force for the agglomeration of Janus particles within the temperature range of LCST. With longer PNIPAM chain on the surface, the onset of LCST upshifts, whereas the temperatures at which all samples reached lowest transmittance are relatively constant. The thermal transition also broadens with a constant onset temperature as the particle concentration decreases.

AUTHOR INFORMATION

Corresponding Author

*E-mail: chrisli@drexel.edu.

Notes

The authors declare no competing financial interest.

ACKNOWLEDGMENTS

This work was partially supported by Army Materials Center of Excellence Program (contract W911NF-06-2-0013) and the NSF (DMR-0804838 and CMMI-1100166). FTIR, SEM, and TEM experiments were carried out at the Drexel's Centralized Research Facility.

REFERENCES

(1) Degennes, P. G. *Rev. Mod. Phys.* **1992**, *64*, 645−648.
(2) Perro, A.; Reculusa, S.; Ravaine, S.; Bourgeat-Lami, E. B.; Duguet, E. *J. Mater. Chem.* **2005**, *15*, 3745−3760.
(3) Glotzer, S. C. *Science* **2004**, *306*, 419−420.
(4) Walther, A.; Muller, A. H. E. *Soft Matter* **2008**, *4*, 663−668.
(5) Manoharan, V. N.; Elsesser, M. T.; Pine, D. J. *Science* **2003**, *301*, 483−487.
(6) Walther, A.; Matussek, K.; Muller, A. H. E. *ACS Nano* **2008**, *2*, 1167−1178.
(7) Walther, A.; Hoffmann, M.; Muller, A. H. E. *Angew. Chem., Int. Ed.* **2008**, *47*, 711−714.
(8) Glotzer, S. C.; Solomon, M. J. *Nat. Mater.* **2007**, *6*, 557−562.
(9) Li, F.; Josephson, D. P.; Stein, A. *Angew. Chem., Int. Ed.* **2011**, *50*, 360−388.
(10) Jiang, S.; Chen, Q.; Tripathy, M.; Luijten, E.; Schweizer, K. S.; Granick, S. *Adv. Mater.* **2010**, *22*, 1060−1071.
(11) Nie, L.; Liu, S. Y.; Shen, W. M.; Chen, D. Y.; Jiang, M. *Angew. Chem., Int. Ed.* **2007**, *46*, 6321−6324.
(12) Wang, B. B.; Li, B.; Dong, B.; Zhao, B.; Li, C. Y. *Macromolecules* **2010**, *43*, 9234−9238.
(13) Gangwal, S.; Pawar, A.; Kretzschmar, I.; Velev, O. D. *Soft Matter* **2010**, *6*, 1413−1418.
(14) Herlihy, K. P.; Nunes, J.; DeSimone, J. M. *Langmuir* **2008**, *24*, 8421−8426.
(15) Gangwal, S.; Cayre, O. J.; Velev, O. D. *Langmuir* **2008**, *24*, 13312−13320.
(16) Kaufmann, T.; Gokmen, M. T.; Wendeln, C.; Schneiders, M.; Rinnen, S.; Arlinghaus, H. F.; Bon, S. A. F.; Du Prez, F. E.; Ravoo, B. J. *Adv. Mater.* **2011**, *23*, 79−83.
(17) Chen, Q.; Whitmer, J. K.; Jiang, S.; Bae, S. C.; Luijten, E.; Granick, S. *Science* **2011**, *331*, 199−202.
(18) Chen, Q.; Bae, S. C.; Granick, S. *Nature* **2011**, *469*, 381−384.
(19) Suzuki, D.; Tsuji, S.; Kawaguchi, H. *J. Am. Chem. Soc.* **2007**, *129*, 8088−8089.
(20) Berger, S.; Synytska, A.; Ionov, L.; Eichhorn, K. J.; Stamm, M. *Macromolecules* **2008**, *41*, 9669−9676.
(21) Isojima, T.; Lattuada, M.; Vander Sande, J. B.; Hatton, T. A. *ACS Nano* **2008**, *2*, 1799−1806.
(22) Schild, H. G. *Prog. Polym. Sci.* **1992**, *17*, 163−249.
(23) Paunov, V. N.; Cayre, O. J. *Adv. Mater.* **2004**, *16*, 788−791.

(24) Lu, Y.; Xiong, H.; Jiang, X. C.; Xia, Y. N.; Prentiss, M.; Whitesides, G. M. *J. Am. Chem. Soc.* **2003**, *125*, 12724−12725.
(25) Koo, H. Y.; Yi, D. K.; Yoo, S. J.; Kim, D. Y. *Adv. Mater.* **2004**, *16*, 274−277.
(26) Reculusa, S.; Poncet-Legrand, C.; Perro, A.; Duguet, E.; Bourgeat-Lami, E.; Mingotaud, C.; Ravaine, S. *Chem. Mater.* **2005**, *17*, 3338−3344.
(27) Perro, A.; Reculusa, S.; Pereira, F.; Delville, M. H.; Mingotaud, C.; Duguet, E.; Bourgeat-Lami, E.; Ravaine, S. *Chem Commun* **2005**, 5542−5543.
(28) Yu, H.; Chen, M.; Rice, P. M.; Wang, S. X.; White, R. L.; Sun, S. H. *Nano Lett* **2005**, *5*, 379−382.
(29) Qiang, W.; Wang, Y.; He, P.; Xu, H.; Gu, H.; Shi, D. *Langmuir* **2008**, *24*, 606−608.
(30) Erhardt, R.; Zhang, M. F.; Boker, A.; Zettl, H.; Abetz, C.; Frederik, P.; Krausch, G.; Abetz, V.; Muller, A. H. E. *J. Am. Chem. Soc.* **2003**, *125*, 3260−3267.
(31) Walther, A.; Andre, X.; Drechsler, M.; Abetz, V.; Muller, A. H. E. *J. Am. Chem. Soc.* **2007**, *129*, 6187−6198.
(32) Nie, Z. H.; Li, W.; Seo, M.; Xu, S. Q.; Kumacheva, E. *J. Am. Chem. Soc.* **2006**, *128*, 9408−9412.
(33) Dendukuri, D.; Pregibon, D. C.; Collins, J.; Hatton, T. A.; Doyle, P. S. *Nat. Mater.* **2006**, *5*, 365−369.
(34) Nisisako, T.; Torii, T. *Adv. Mater.* **2007**, *19*, 1489−1493.
(35) Yin, Y. D.; Lu, Y.; Gates, B.; Xia, Y. N. *J. Am. Chem. Soc.* **2001**, *123*, 8718−8729.
(36) Yin, Y. D.; Lu, Y.; Xia, Y. N. *J. Am. Chem. Soc.* **2001**, *123*, 771−772.
(37) Roh, K. H.; Martin, D. C.; Lahann, J. *Nat. Mater.* **2005**, *4*, 759−763.
(38) Roh, K. H.; Martin, D. C.; Lahann, J. *J. Am. Chem. Soc.* **2006**, *128*, 6796−6797.
(39) Roh, K. H.; Yoshida, M.; Lahann, J. *Langmuir* **2007**, *23*, 5683−5688.
(40) Kim, J. W.; Larsen, R. J.; Weitz, D. A. *J. Am. Chem. Soc.* **2006**, *128*, 14374−14377.
(41) Tang, C.; Zhang, C. L.; Liu, J. G.; Qu, X. Z.; Li, J. L.; Yang, Z. Z. *Macromolecules* **2010**, *43*, 5114−5120.
(42) Rao, T.; Dong, X.-H.; Katzenmeyer, B. C.; Wesdemiotis, C.; Cheng, S. Z. D.; Becker, M. L. *Soft Matter* **2012**, *8*, 2965−2971.
(43) Hong, L.; Jiang, S.; Granick, S. *Langmuir* **2006**, *22*, 9495−9499.
(44) Liu, B.; Wei, W.; Qu, X.; Yang, Z. *Angew. Chem., Int. Ed.* **2008**, *47*, 3973−3975.
(45) Liu, B.; Zhang, C. L.; Liu, J. G.; Qu, X. Z.; Yang, Z. Z. *Chem Commun* **2009**, 3871−3873.
(46) Wang, Y.; Zhang, C.; Tang, C.; Li, J.; Shen, K.; Liu, J.; Qu, X.; Li, J.; Wang, Q.; Yang, Z. *Macromolecules* **2011**, *44*, 3787−3794.
(47) Li, C. Y. *J. Polym. Sci., Polym. Phys.* **2009**, *47*, 2436−2440.
(48) Chen, W. Y.; Li, C. Y.; Zheng, J. X.; Huang, P.; Zhu, L.; Ge, Q.; Quirk, R. P.; Lotz, B.; Deng, L.; Wu, C.; Thomas, E. L.; Cheng, S. Z. D. *Macromolecules* **2004**, *37*, 5292−5299.
(49) Chen, W. Y.; Zheng, J. X.; Cheng, S. Z. D.; Li, C. Y.; Huang, P.; Zhu, L.; Xiong, H.; Ge, Q.; Guo, Y.; Quirk, R. P.; Lotz, B.; Deng, L.; Wu, C.; Thomas, E. L. *Phys. Rev. Lett.* **2004**, *93*, 028301.
(50) Wang, B. B.; Li, B.; Xiong, J.; Li, C. Y. *Macromolecules* **2008**, *41*, 9516−9521.
(51) Li, B.; Li, L. Y.; Wang, B. B.; Li, C. Y. *Nat. Nanotechnol.* **2009**, *4*, 358−362.
(52) Wang, B. B.; Li, B.; Zhao, B.; Li, C. Y. *J. Am. Chem. Soc.* **2008**, *130*, 11594−11595.
(53) Wang, B. B.; Dong, B.; Li, B.; Zhao, B.; Li, C. Y. *Polymer* **2010**, *51*, 4814−4822.
(54) Li, B.; Li, C. Y. *J. Am. Chem. Soc.* **2007**, *129*, 12−13.
(55) Li, B.; Ni, C.; Li, C. Y. *Macromolecules* **2008**, *41*, 149−155.
(56) Li, B.; Wang, B. B.; Ferrier, R. C. M.; Li, C. Y. *Macromolecules* **2009**, *42*, 9394−9399.
(57) Wang, B. B.; Li, B.; Ferrier, R. C. M.; Li, C. Y. *Macromol. Rapid Commun.* **2010**, *31*, 169−175.
(58) Dong, B.; Li, B.; Li, C. Y. *J. Mater. Chem.* **2011**, *21*, 13155−13158.
(59) De, M.; Ghosh, P. S.; Rotello, V. M. *Adv. Mater.* **2008**, *20*, 4225−4241.
(60) Burns, A.; Ow, H.; Wiesner, U. *Chem. Soc. Rev.* **2006**, *35*, 1028−1042.
(61) Zhang, J.; Jin, J.; Zhao, H. Y. *Langmuir* **2009**, *25*, 6431−6437.
(62) Paoletti, P.; Ciampolini, M.; Sacconi, L. *J Chem Soc* **1963**, 3589−3593.
(63) Li, D.; Sheng, X.; Zhao, B. *J. Am. Chem. Soc.* **2005**, *127*, 6248−6256.
(64) Costa, T. M. H.; Gallas, M. R.; Benvenutti, E. V.; daJornada, J. A. H. *J. Non-Cryst. Solids* **1997**, *220*, 195−201.
(65) Ejaz, M.; Ohno, K.; Tsujii, Y.; Fukuda, T. *Macromolecules* **2000**, *33*, 2870−2874.
(66) Hu, H.; Dorset, D. L. *Macromolecules* **1990**, *23*, 4604−4607.
(67) Wu, T.; Zhang, Y.; Wang, X.; Liu, S. *Chem. Mater.* **2007**, *20*, 101−109.
(68) Lattuada, M.; Hatton, T. A. *J. Am. Chem. Soc.* **2007**, *129*, 12878−12889.